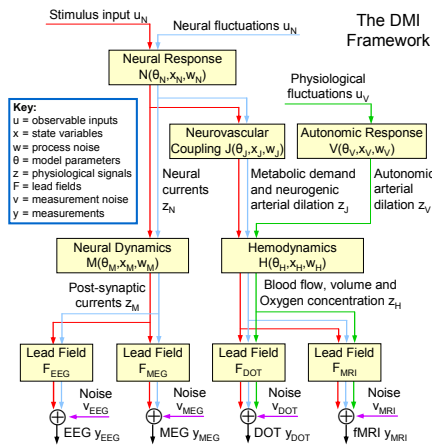


A State-Space Framework for Functional Neuroimaging

Solomon Gilbert Diamond, Theodore J. Huppert, Patrick L. Purdon, Steven M. Stufflebeam, Giorgio Bonmassar, Matti S. Hämäläinen, Emery N. Brown, David A. Boas
 MGH/MIT/HMS Athinoula A. Martinos Center for Biomedical Imaging, Charlestown, Massachusetts, 02129, USA

The DMI Framework

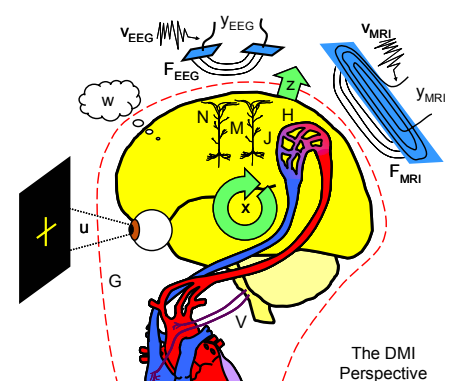


Introduction

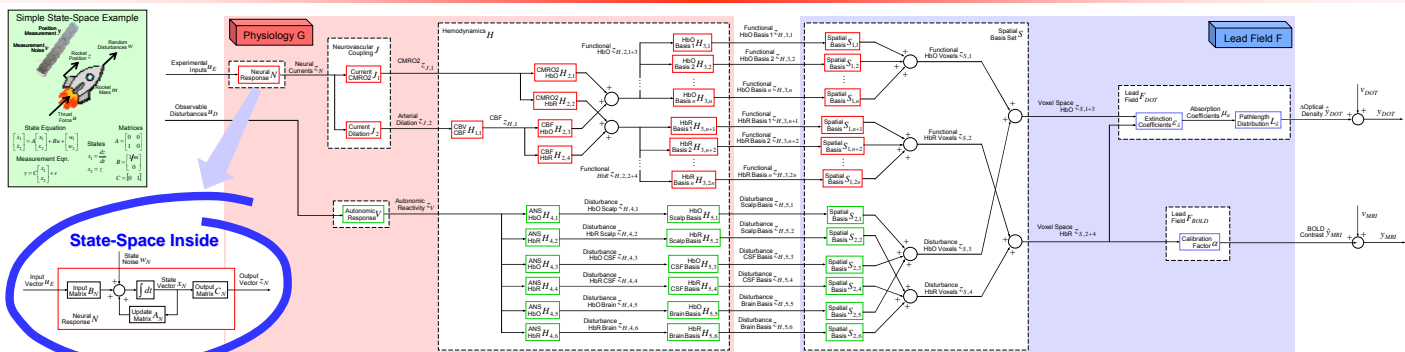
A physiologically-based system model of the human brain offers exciting advantages when analyzing concurrent measurements from multiple functional neuroimaging modalities because a common set of physiological states and parameters could define the system. Dynamic state observers and system identification tools from modern control theory could then optimize spatiotemporal resolution and improve estimates of causal relationships. The migration of modeling and analysis techniques to a common state-variable framework would facilitate this process while also speeding collaboration and the sharing of computational resources. These advantages are not currently realized in the neuroimaging community. The strategy of organizing a system model of the vastly complex, multiscale and dynamic human brain may appear particularly daunting. We argue, however, that the design process can begin now with a state-variable analysis framework that does not prescribe the details of anatomical and physiological models. Once the framework is established, many existing analysis schemes could be directly transformed into state-variable subsystems.

Of particular practical interest is improving the spatiotemporal resolution and physiological accuracy of multimodal functional neuroimaging with concurrent measurements. Significant attention has been applied to fusing electroencephalogram (EEG) and functional magnetic resonance imaging (fMRI) because of their complementary temporal and spatial resolutions (see Valdes-Sosa 2005 for a review). Another spatiotemporal resolution pair is diffuse optical tomography (DOT) with fMRI (Hoge et al. 2005), which improves physiological accuracy. The electromagnetic perspective combines EEG with magnetoencephalography (MEG). Other technically feasible combinations are DOT with EEG and DOT with MEG. Multimodal techniques have been applied to address the spatiotemporal evolution of neuronal activation (Eichele et al. 2005), the neuronal basis of the fMRI signal (Babajani et al. 2005) and functional connectivity (Rabibi et al. 2005). Clinical applications of multimodal functional neuroimaging include Alzheimer's disease (Kilhy et al. 2005), dyslexia (Grunling et al. 2004), epilepsy (Gottman et al. 2004) and pain (Lannetti et al. 2005).

Modern control theory offers a toolset that is ideally suited to multimodal integration in functional neuroimaging. Kalman and his colleagues transformed the field of control theory between 1960 and 1961 with a series of groundbreaking papers (Kalman and Bucy 1961). They proposed a time-domain approach using linear algebra and state variables that is well suited to time-varying linear and nonlinear systems, multiple-input, multiple-output (MIMO) systems and describing the internal dynamics of systems. Modern control theory is valued across the engineering disciplines for its proven robustness, optimality and stability. Related dynamic analysis methods have been applied to fMRI (Riera et al. 2004), DOT (Diamond et al. 2005) and EEG (Gulka et al. 2004) demonstrating improved resolution, dynamic signal tracking and physiological modeling. The widespread entry of modern control theory into functional neuroimaging would be greatly enhanced by a general purpose state-variable model of the brain.



DMI Applied to DOT and fMRI BOLD



Model Configuration for DOT-BOLD

Our purpose at this stage of model development was to test the basic functionality of the DMI framework. Of primary concern was to evaluate the numerical stability and computational demands of a real multimodal data set with a continuous-time dynamical model. Our results indicate the feasibility of DMI analysis. Evaluation of whether this particular model configuration can provide superior results when compared with other analysis methods will be determined later.

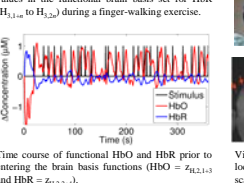
We used a single functional pathway to describe the neurovascular response to the stimulus consisting of a series of 2nd order ordinary differential equations (ODEs) in the neural response N , neurovascular coupling J and hemodynamics H functions. These functions were parameterized by adjusting the undamped natural frequencies and damping ratios somewhat arbitrarily until a simulated hemodynamic timecourse appeared reasonable. Next the hemodynamics pass through a parallel array of 194 1st order ODEs for HbO and another 194 for HbR in the brain, one for each functional spatial basis. These 1st order ODEs allow each basis to apply a different gain and time constant to the hemodynamic signals that pass through. There are a total of 404 states associated with the functional response.

The background physiology was modeled with process noise that goes through a 2nd order low pass autoregressive response system V . A gain and phase shift is then introduced for the global skin, CSF and brain voxels within the hemodynamics H function. This configuration allows for incorporating prior knowledge about the frequency dependent gain and phase dynamics introduced by cerebral autoregulation. A total of 20 states were associated the background physiology.

We successfully precomputed the Kalman gain matrix L in about an hour on a modern 64-bit desktop PC with 16 GB of RAM. Performing the state estimation with the continuous-time Kalman-Bucy filter then ran in about 15 minutes. No problems with numerical stability were encountered. Least squares system identification was then performed on the subsystems. While the present results demonstrate feasibility of the method, additional work is needed to test the accuracy of the physiological estimates. The next steps include setting all the model parameters to best fit the data, which provides a direct measure of model fit. We will then use the model to predict the data and to set the process noise variance to reflect our confidence in different aspects of the model.

Experimental Methods

DOT Protocol
 Continuous wave (CW) optical measurements were made at 690nm and 830nm. Data was converted to optical density prior to being used in the model. Optical measurements were down-sampled to 2Hz for fusion with the fMRI data set.



Subjects

We performed simultaneous DOT and BOLD imaging on 5 healthy, right-handed subjects while they performed a rapid event-related finger-walking exercise. This data has been published in Huppert et al (2006).

fMRI Protocol

GE-EPI BOLD was collected using a 3T Allegra scanner (TR/TE/FA = 500ms/30ms/90°). The in-plane resolution was 3.75mm and five 6mm oblique slices (1mm gap) were acquired. A MPRAGE scan was acquired and segmented into a layered head model (skin, skull, CSF, gray/white). Photon Migration Monte Carlo simulations were performed to determine the light propagation through tissue-segmented anatomical volumes for each subject. These were used to create the optical forward models (i.e. sensitivity functions) for each source-detector measurement pair.

Calibrating the BOLD signal

The BOLD calibration factor (α) is pre-computed by first projecting the BOLD signal through the DOT forward equation. This accounts for the partial-volume and path-length effects of the optical measurements. The BOLD-generated HbR change is then compared of the optical measurements in order to calculate the calibration factor. This method has been described in Huppert et al. (175 W-AM) as a way of spatially correlating the two methods.

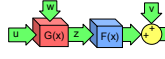
Spatial Basis Functions

Each subject is anatomically segmented into the five tissue types. The superficial layers are grouped in order to model global fluctuations.

Theoretical Development

DMI Forward Model

Dynamic multimodal integration (DMI) is a multiscale-system framework for dynamic functional modeling and multimodal integration. The central aspect of DMI is that a common neurovascular system model G produces the physiological signals z , which are observed through the lead field biophysics F of each imaging modality.



On its largest scale lead field function F and physiological forward model G define the functional relationship between an input vector u and the neuroimaging measurements y . The inputs u can include controllable experimental stimuli like the timing and events in a functional paradigm and observable disturbances like blood pressure variations and background neural fluctuations. Unobservable disturbances w and measurement noise v are modeled stochastically.

Physiology Function G

The physiology function G predicts the dynamic physiological signals z with a cascade of functions that model specific biological processes. The neural response function N models how the neural currents in the brain z_N respond to experimental input u_N and observable disturbances w_N . The neural response function N could represent the arrangement of the neural subsystem as found in a dynamic causal model (Friston et al. 2003). The neural currents z_N are related to the post-synaptic currents z_M by the neural dynamics function M . The hemodynamics function H models cerebral arterial dilation z_V due to autonomic regulatory activity, this component of the signal z_V is separately modeled by the autonomic response function V . The hemodynamic function H models cerebral arterial dilation z_V due to autonomic regulatory activity, this component of the signal z_V is separately modeled by the autonomic response function V . The hemodynamic function H models cerebral arterial dilation z_V due to autonomic regulatory activity, this component of the signal z_V is separately modeled by the autonomic response function V .

Lead Field Function F

The biophysics of the imaging modalities is captured in the lead field functions F . The F_{EEG} and F_{MEG} lead fields estimate electric and magnetic fields at the scalp surface generated by post-synaptic currents in the brain (Hämäläinen et al. 1993; Nunez et al. 1994). The F_{DOT} lead field estimates the photon fluorescence based on the scalp surface generated by an arrangement of laser sources (Okada et al. 1996; Boas et al. 2002). The specifics of the F_{fMRI} lead field are dependent on the particular scanning procedure used. Blood oxygen level dependent (BOLD) signal contrast derives largely from fractional venous blood volume (fBV) from oxygen venous blood volume and deoxyhemoglobin content (Ogawa et al. 1993; Ohta et al. 2004). Another example is arterial spin labeling (ASL) perfusion fMRI, which provides a direct measure of cerebral blood flow (CBF) by using the water in arterial blood as an endogenous tracer (Detre et al. 1994). It is possible with fMRI to interleave the different scanning sequences making the F_{fMRI} lead field dependent on the specific acquisition time.

State-Variable Models

The state-variable model is a generic form for describing dynamic systems with input U , output C and state A matrices.

Although we illustrate the continuous-time, linear, time-invariant version, the same general model structure can handle discrete-time, nonlinear and time-varying systems. The unique characteristic of state-variables is that given known inputs and disturbances, they are a minimum representation of the full system behavior at all future time (Kuo 1995). Although the states are often not directly measured, they may still be observable based on the input-output behavior of the system. The state-variable models thus provide explicit access to the internal system dynamics and their functional relationship with output behavior. Exploiting these relationships is a key element of optimal estimation and multimodal integration.

Unifying State-Variable Subsystems

Our objective is to express the network of physiological subsystems into a single state-variable model of the form

$$\dot{x} = Ax + Bu + w$$

$$y = Cx + v$$

The input vector u contains the experimental inputs and disturbances

$$u = [u_1 \dots u_p]^T$$

The state x and state noise w vectors are the concatenated column vectors from the subsystems

$$x = [x_1 \dots x_n \dots x_N]^T$$

$$w = [w_1 \dots w_n \dots w_N]^T$$

A similar concatenation is performed on the measurements y and measurement noise v

$$y = [y_{1,1} \dots y_{1,n} \dots y_{N,1} \dots y_{N,n}]^T$$

$$v = [v_{1,1} \dots v_{1,n} \dots v_{N,1} \dots v_{N,n}]^T$$

State Estimation

The continuous-time Kalman-Bucy filter

$$\dot{\hat{x}} = A\hat{x} + Bu + L(y - C\hat{x})$$

is the optimal recursive observer for linear state-variable models. The observer gain L is optimal when

$$L = PC^T R^{-1}$$

the estimated state error covariance P is obtained by solving the Riccati equation

$$\dot{P} = PA^T + AP + Q - PC^T R^{-1} CP$$

and Q and R are the covariances of w and v respectively.

References

Babajani, A. M.H., Nohales, and H. Soliman-Zadeh, Integrated MEG and fMRI model: Systematic analysis. *Brain Topography*, 2005, 18(2): 101-113.

Bahmani, F. et al. 2005. Estimation of the cortical connectivity with the multimodal integration of EEG and fMRI data by discrete vector field function. *NeuroImage*, 24(1): 118-131.

Boas, D.A., Culver, J., Scott, J., Dunn, A.K., 2003. The dimensional Monte Carlo code for photon migration through complex heterogeneous media including the adult head. *Opt. Express*, 10, 179-193.

Boas, R. A., Wang, K. C., Frank, L. R., 1998. Dynamics of blood flow and oxygenation changes during brain activation: The balloon model. *Brain Reson. Method*, 9(6): 85-88.

Danzon, J. et al. 1994. True-positive perfusion imaging using arterial spin-labeling. *MRI in Biomed*, 7(1-2): 75-82.

Diamond, S.G., Huppert, T.J., Kolemnik, V., Fruehlich, M.A., Kipnis, J.P., Amidei, S.R., and Boas, D.A., 2006. Dynamic physiological modeling for functional diffuse optical tomography. *NeuroImage*, 30(3): 818-830.

Eichele, T. et al. Assessing the spatiotemporal evolution of neuronal activation with single-trial event-related potentials and functional MRI. *Proceedings of the National Academy of Sciences of the United States of America*, 2005, 102(12): 6173-6178.

Engel, S.A., Glover, G.H., Wandell, B.A., 1997. Retinotopic cortical mapping of visual spatial frequency and orientation selectivity. *Journal of Neurophysiology*, 77(6): 288-307.

Gulka, A., Yamashita, H., Frank, T., Hoge, R., Valdes-Sosa, P., 2004. A solution to the inverse problem of EEG generation using spatiotemporal Kalman filtering. *NeuroImage*, 21, 435-453.

Gutman, S. C.G., 2005. *Control of Brain-Eeg and MEG in Epilepsy: Methodological, clinical and clinical studies*. Combining EEG and MEG in Epilepsy. *Methodological, clinical and clinical studies*. Combining EEG and MEG in Epilepsy. *Methodological, clinical and clinical studies*.

Hämäläinen, M. et al. 1993. The possibility of noninvasive magnetic integration of MEG and fMRI to study the functional organization of the human brain. *NeuroImage*, 10(2): 117-126.

Hämäläinen, M., Hari, R., Ilmoniemi, R. J., Knuttila, J., Lounasmaa, O. V. 1993. Magnetoencephalography: theory, instrumentation, and applications in noninvasive studies of the working human brain. *Rev. Modern Physics*, 65(2): 413-497.

Hoge, R.D., et al. Simultaneous recording of task-induced changes in blood oxygenation, volume, and flow using diffuse optical imaging and arterial spin-labeled MRI. *NeuroImage*, 2005, 25(3): 701-707.

Jennrich, G.D., et al. Simultaneous recording of task-evoked brain potentials and continuous, high-field functional magnetic resonance imaging in humans. *NeuroImage*, 2005, 26(2): 370-379.

Kalman, R. E., Bucy, R. S., "New Results in Linear Filtering and Prediction Theory". *Intelligence from Systems: Journal of Basic Engineering*, Vol. 82, pp. 107-116(1961).

Kelly, K.A., et al. Detection of vascular amyloid-beta deposition using a novel PET tracer, AV-45. *Journal of Neurology*, 2005, 252(1): 127-136.

Kuo, B. C. 1995. *Automatic Control Systems*. Upper Saddle River, NJ: Prentice Hall.

Mandelkern, J. B. et al. 1999. Evidence of a cardiovascular pathway subserved with delayed compliance. *J. Cereb. Blood Flow Metab.*, 19(6): 679-689.

Nunez, P. L., et al. 1994. A theoretical and experimental study of high-resolution core based on surface topography and cortical imaging. *EEG and Clin. Neurophys.*, 90(1): 40-57.

Ohata, T., et al. 2004. Discrepancies between BOLD and flow dynamics in primary and secondary motor areas: applications of the balloon model to the interpretation of BOLD transients. *NeuroImage*, 21, 144-153.

Ogawa, S., et al. 1993. Functional brain mapping by blood oxygenation dependent contrast: magnetic resonance imaging of a canine model with a biological model. *Biophys. J.*, 64, 805-812.

Okada, E., Scholinger, M., Widge, S.R., Peltola, M., Delopy, D.T., 1996. Experimental validation of Monte Carlo and finite-element methods of estimation of the optical pathlength in absorptionless media. *Appl. Opt.*, 35(10): 1362-1371.

Valdes-Sosa, P.A., et al. 2004. A state-space model of the hemodynamic response nonlinear interaction between blood flow and oxygenation. *NeuroImage*, 21, 1457-1467.

Valdes-Sosa, P.A., R. Kotte, and K.J. Friston, 2005. Introduction: multimodal functional neuroimaging. *Philosophical Transactions of the Royal Society B: Biological Sciences*, 360(1457): 865-867.